VI.4. FISCHER-TROPSCH SYNTHESIS: IMPACT OF POTASSIUM AND ZIRCONIUM PROMOTERS ON THE ACTIVITY AND STRUCTURE OF AN ULTRAFINE IRON OXIDE CATALYST (Robert J. O'Brien, Liguang Xu, Diane R. Milburn, Yong-Xi Li, Kenneth J. Klabunde and Burtron H. Davis)

VI.4.1. ABSTRACT

Slurry phase Fischer-Tropsch synthesis was conducted with an ultrafine iron oxide catalyst promoted with either 0.5 atomic % K or 1.0 atomic % Zr or both. Pretreatment in CO yielded higher conversions and a more stable catalyst than activation in hydrogen or synthesis gas. Hydrogen pretreatment of K promoted catalysts and synthesis gas activation in general were less effective. Mössbauer spectroscopy and XRD showed χ-Fe_5C_2 and ϵ'-$Fe_{2.2}C$ were formed during pretreatment in CO and did not depend on promoters present. Catalysts pretreated in H_2 were reduced to metallic Fe and Fe_3O_4; promotion with K and Zr decreased the extent of reduction. Hydrogen pretreated catalysts, promoted with K, lost surface area and carbided rapidly under synthesis conditions. Activation in synthesis gas reduced all catalysts to Fe_3O_4. Subsequent synthesis did not effect the phase present for the unpromoted and Zr promoted catalysts while those promoted with K formed χ-Fe_5C_2 and ϵ'-$Fe_{2.2}C$. It is concluded that pretreatment type is more important to the catalyst activity during the early period of synthesis than the impact of promotion with K and/or Zr and that changes in the bulk composition of iron catalysts do not necessarily correlate with changes in activity.

VI.4.2. INTRODUCTION

Promoters have a large effect on the activity and selectivity of iron Fischer-Tropsch (FT) catalysts (VI.4.1). Alkali promoters, and K in particular, have been well established as a means of increasing olefin selectivity, producing high molecular weight products and increasing the activity of iron catalysts (VI.4.2,VI.4.3). Promoters also impact the physical properties of iron FT catalysts. Potassium has been shown to increase the rate of iron carbide formation and carbon deposition during the FT synthesis (VI.4.4) and it is known to decrease the surface area of iron catalysts (VI.4.5). Nonreducible oxides of Si, Al, Ti, Mg, Zn and Th have been utilized as structural promoters to stabilize the surface area and extend the life of FT catalysts (VI.4.1,VI.4.6). Structural promoters are also reported to influence the type of iron carbide formed during the FT synthesis (VI.4.7) and have been shown to inhibit the reduction of iron catalysts during pretreatment (VI.4.6).

Pretreatment conditions and type can also impact the activity and phase transformations of iron catalysts (VI.4.8). Activation of Fe catalysts is more complicated than that of Ru and Co catalysts. Standard pretreatment of Ru and Co has involved reduction of the catalysts in H_2 to the zero valent state. Pretreatment in H_2 has proven to be necessary to activate fused Fe_3O_4 catalysts (VI.4.1), whereas activation in CO is effective for precipitated catalysts (VI.4.2,VI.4.9). Precipitated catalysts have also been successfully activated in synthesis gas at 280°C (VI.4.10). Regardless of the pretreatment conditions, a mixture of iron carbides and oxides form during the FT synthesis (VI.4.11). Iron carbides reported to form are ϵ'-$Fe_{2.2}C$, χ-Fe_5C_2, θ-Fe_3C (VI.4.12) and Fe_7C_3 (VI.4.13). Magnetite is usually formed during the

FT synthesis particularly when activity is high and H_2O/H_2 and CO_2/CO ratios are high enough to oxidize the iron carbides (VI.4.14).

Ultrafine particles have been defined to have sizes less than 0.1 μm in contrast to precipitated catalysts which have agglomerate sizes greater than 1 μm. Itoh et al. have reported on various ultrafine metallic iron catalysts with particle sizes less than 0.1 μm (VI.4.15,VI.4.16,VI.4.17,VI.4.18). They found that UFP catalysts have activities much greater than precipitated catalysts and have a higher selectivity for olefins.

Recently we have reported results on a commercially available ultrafine Fe_2O_3 catalyst that has an average particle size of 30 Å (VI.4.19,VI.4.20). Mössbauer spectroscopy showed that the catalyst activated in H_2 followed by synthesis converts the catalyst to Fe_3O_4 and a small amount of ϵ'-$Fe_{2.2}C$ and θ-Fe_3C. Pretreatment in CO fully reduced the catalyst to χ-Fe_5C_2; however, 72 hr of synthesis oxidized the catalyst to 100% Fe_3O_4. It was of interest to learn what effect promoters have on this ultrafine catalyst composition and activity. Previously we reported on a precipitated iron catalyst promoted with 6 wt % ThO_2 (VI.4.21). Promotion with ThO_2 was common with commercial cobalt catalysts and has been reported by Dry to increase the activity of a $Fe/Cu/SiO_2$ catalyst (VI.4.1); however, ThO_2 is not currently an acceptable promoter for commercial catalysts because of environmental concerns about its radioactivity. Promotion with ZrO_2 is a plausible substitute for ThO_2 due to their similar activities for the iso synthesis (VI.4.22) and the dehydration of alcohols (VI.4.23,VI.4.24). Herein is reported the Mössbauer, XRD and BET characterization of a 30 Å iron oxide catalyst promoted with K and/or ZrO_2 and subjected to slurry phase FT synthesis.

VI.4.3. EXPERIMENTAL

VI.4.3.a. Catalyst Activation and Process Conditions

A process scheme similar to that reported previously (VI.4.19) was utilized in the current study. A 10.0 g sample of ultrafine α-Fe_2O_3 (MACH I Inc., 30 Å, ~265 m^2/g) and 140 g of C_{30} polyalphaolefins oil (Ethyl Corporation) were thoroughly mixed in a 300 ml autoclave. Promoters were added directly to the slurry in the form of potassium t-butoxide or zirconium n-propoxide. Four catalysts with the following compositions, in atomic % relative to Fe, were used: 100Fe, 100Fe/0.5K, 100Fe/1.0Zr and 100Fe/0.5K/1.0Zr. The catalyst slurry was heated to 260°C at 1.5-2.0°C/min at 100 psig while pretreatment gas (H_2 or CO) or synthesis gas (H_2/CO=1) was introduced into the reactor at a flow rate of 3.0 nL/hr/g-Fe. After reaching 260°C, the flow of pretreatment gas was continued for 24 hr. Synthesis gas (H_2/CO=1) was then started at a flow rate of 3.0 nL/hr/g-Fe. Catalyst slurry samples were removed (~10-15 g containing about 0.7 g catalyst) from the reactor at various times of the pretreatment and synthesis runs. CO and H_2 conversions were determined by analyzing the exit gas stream with a Carle gas analyzer. Catalyst slurry samples were stirred in tetrahydrofuran or cyclohexane (~250mL) at room temperature to dissolve the reactor wax and oil. The catalyst samples were then filtered, and dried at room temperature under vacuum. Catalyst samples selected for analysis were Soxhlet extracted with refluxing toluene to remove traces of wax in the catalyst pores.

VI.4.3.b. Catalyst Analysis

Mössbauer Spectroscopy. Mössbauer spectra of the catalyst samples were obtained from a constant acceleration spectrometer. The γ-ray source consisted of

50-100 mCi of ^{57}Co in a Pd matrix. Spectra were analyzed using a least-squares fitting routine with the iron content of each phase determine from their relative peak areas.

X-ray Diffraction. Powder X-ray diffraction patterns of the catalysts were obtained using a Philips APD X-ray diffraction spectrometer equipped with a Cu anode and Ni filter operated at 40 Kv and 20 Ma (CuKα = 1.5418 Å). Iron phases were identified by comparing diffraction patterns of the catalyst samples with those in the standard powder X-ray diffraction file compiled by the Joint Committee on Powder Diffraction Standards published by the International Center for Diffraction Data.

BET Surface Area Determination. Nitrogen adsorption measurements were made with a Quantachrome Autosorb 6 instrument. Samples were outgassed at 80°C and less than 50 mtorr for a minimum of 12 hr prior to analysis. BET surface areas and pore size distributions were calculated from the adsorption and desorption data, respectively.

VI.4.4. RESULTS

VI.4.4.a. Catalyst Activity

Unpromoted catalyst, 100Fe. In our initial FT study with this catalyst, it was reported that CO pretreatment leads to a catalyst activity three times that of hydrogen pretreated or synthesis gas activated catalysts (VI.4.19). Tetralin was used as the start-up solvent in that study and a reflux condenser was needed to prevent evaporation of the tetralin. It was found that the condenser enabled water to accumulate in the reactor which caused the metallic iron formed by H_2 pretreatment to sinter. In a subsequent study, a Dean-Stark condenser was used to eliminate water from the reactor and it was found that CO and H_2 pretreatments led to similar FT

activity (VI.4.20). A less volatile start-up solvent was used in the present study which eliminated the need for a reflux condenser. Pretreatment of the unsupported catalyst in CO (Figure VI.4.1) led to an initial activity slightly higher than that of the H_2 pretreated catalyst; however, after 72 hr of synthesis, the total synthesis gas conversions were about the same. These results reproduce those of our second study (VI.4.20). As was reported earlier, activation in synthesis gas proved to be ineffective for this catalyst.

Potassium promoted catalyst, 100Fe/0.5K. CO pretreatment of this catalyst gave the best activity and stability (Figure VI.4.1). Synthesis gas activation led initially to a much higher conversion of about 68%; however, within 24 hr, the activity had dropped to below 30% conversion. The conversion for the catalyst pretreated in CO was very stable at approximately 32% throughout the run. The catalyst pretreated in H_2 was much less active; its initial conversion of 20% dropped to below 5% after 24 hr of synthesis.

Zirconium promoted catalyst, 100Fe/1.0Zr. CO pretreatment of the zirconium promoted catalyst resulted in the most active and stable catalyst of the ones used in this study (Figure VI.4.1). The initial conversion exceeded 50%; however, an induction period was evident as the conversion rose to above 60% after 24 hr of synthesis. The conversion eventually decreased to 42% after 48 hr where it remained until the end of the run. Hydrogen pretreatment of this catalyst resulted in a conversion between 25% and 30% throughout the 72 hr run. Synthesis gas activation gave a catalyst with very low stability; initially the conversion was greater than 25%; however, it dropped to below 5% after 24 hr of synthesis.

Doubly promoted catalyst, 100Fe/0.5K/1.0Zr. As was the case for the other three series, CO pretreatment was superior for the doubly promoted catalyst; the conversion rose from 30% to 43% after 48 hr of synthesis (Figure VI.4.1). Hydrogen pretreatment was ineffective since conversions for this run began at 10% and then dropped to 5%. The synthesis gas activation gave a catalyst with a very low initial conversion; however, after 48 hr on stream the conversion rose to 25% before decreasing to 20% after 72 hr of synthesis.

In general, the pretreatment gas seems to have more of an effect on the conversion than the promoters. The zirconium promoted catalyst was much more active than the potassium promoted catalyst in the hydrogen pretreated series. The zirconium promoted catalyst had an initial conversion higher than the other catalysts in the CO pretreated series; nevertheless, after 48 hr the conversions for all of these catalysts were approximately the same. The conversions for all of the catalysts activated in synthesis gas were initially low; only the doubly promoted catalyst activated to any degree in this series.

VI.4.4.b. BET Surface Area and Porosity

The surface area of the unpromoted catalyst as received from the vendor is approximately 265 m^2/g. However, the surface area that is measured strongly depends upon the dehydration procedure, and may vary widely from this value. In every catalyst series of this study, the surface area rapidly declined during the activation period. By the end of all of the activation periods, the surface area of the activated material was never higher than 75 m^2/g.

In general, CO pretreatment resulted in a higher surface area than hydrogen pretreatment or synthesis gas activation for each promoter series (Figure VI.4.2). For the CO pretreated series, the catalysts promoted with zirconium had the highest surface areas; both catalysts containing Zr had surface areas which were approximately 70 m^2/g throughout their respective runs. The unpromoted and K promoted catalysts had nearly identical surface areas which were above 60 m^2/g after pretreatment and they slowly decreased to about 30 m^2/g after 240 hr of synthesis. Hydrogen pretreatment of the unpromoted and zirconium promoted catalysts resulted in surface areas of 30 m^2/g. Subsequent synthesis did not lower the surface areas for 72 hr of synthesis. Hydrogen pretreatment of the potassium promoted catalyst and the doubly promoted catalyst gave essentially the same surface area of about 30 m^2/g; however, the addition of synthesis gas caused the surface areas of these catalysts to decrease to below 10 m^2/g. Exposure of the iron oxide directly to synthesis gas caused the surface area of the unpromoted catalyst to drop to 62 m^2/g after only 3 hr; the surface area then slowly declined to 45 m^2/g after 24 hr and then to 32 m^2/g after 96 hr of exposure. The zirconium promoted catalyst behaved similarly. The potassium promoted catalyst lost surface area more quickly when activated in synthesis gas. After 27.5 hr of exposure, the surface area was 28 m^2/g where it remained until the end of the run at 72 hr. The doubly promoted catalyst behaved like the unpromoted and zirconium promoted catalysts for the first 24 hr of exposure to synthesis gas; however, its surface area quickly decreased towards the end of the run to about 8 m^2/g.

VI.4.4.c. X-ray Diffraction

CO Pretreatment. The phase composition obtained from the x-ray diffraction patterns of all catalysts series pretreated with CO were very similar. All catalysts were rapidly converted to Fe_3O_4 during the heat up period of the activation; however, the conversion to carbide proceeded much slower. After 3-4 hr of the CO pretreatment the 400 line of Fe_3O_4 became broad and grew in intensity. This is attributed to the formation of various iron carbides. After 24 hr of pretreating at process conditions, peaks attributable to Fe_3O_4 were greatly diminished. The carbides χ-Fe_5C_2 and ϵ'-$Fe_{2.2}C$ were definitely present and several lines which can be assigned to θ-Fe_3C were also present. The absence of the 113 and 122 lines of θ-Fe_3C may indicate that the pseudo θ-Fe_3C phase described in other works (VI.4.1) was present. Exposure to synthesis gas caused the carbides to be converted to Fe_3O_4 (Figure VI.4.3). Within 72 hr of synthesis, XRD showed all of the catalysts had been converted to Fe_3O_4, except for the K+Zr promoted catalyst which showed some χ-Fe_5C_2 and ϵ'-$Fe_{2.2}C$. The unpromoted and K promoted catalysts did recarbide to a small extent after 240 hr of synthesis.

Hydrogen Pretreatment. Hydrogen pretreatment gave nearly identical results for all four catalyst series studied. Exposure to H_2 during the heat up period produced a large amount of Fe_3O_4; however, a very small amount of α-Fe_2O_3 was also present. After 24 hr at pretreatment conditions, Fe_3O_4 and α-Fe were the only phases present. Exposure to synthesis gas converted all of the α-Fe to χ-Fe_5C_2 and ϵ'-$Fe_{2.2}C$ for each catalyst. The catalysts without K showed mostly Fe_3O_4 through out the 72 hr of synthesis; however, the unpromoted catalyst began to carbide by the end of the run.

The two catalysts containing K showed the formation of large amounts of ϵ'-$Fe_{2.2}C$ and χ-Fe_5C_2 within 3.5 hr of synthesis; after 24 hr of synthesis, both had been completely carbided.

Synthesis gas Activation. All catalysts were rapidly converted to Fe_3O_4 during the heat-up to 260°C under synthesis gas. Additional exposure to synthesis gas did not change the composition of the unpromoted and zirconium promoted catalysts. The doubly promoted catalyst showed only Fe_3O_4 during the first 48 hr of synthesis gas exposure; however, it rapidly carbided over the next 48 hr to χ-Fe_5C_2 and ϵ -$Fe_{2.2}C$ leaving only a small amount of Fe_3O_4. The K promoted catalyst began to form χ-Fe_5C_2 and ϵ'-$Fe_{2.2}C$ within the first 24 hr of synthesis gas exposure and within 96 hr had been completely carbided.

VI.4.4.d. Mössbauer Spectroscopy

CO Pretreatment. The Mössbauer spectroscopy results closely parallel the XRD results. All four catalyst series appeared to form small particle Fe_3O_4 during the heat-up period and the first 3 hr of pretreatment at process conditions. This was evident by very broad spectra which were probably the result of a wide range of particle sizes. Pretreatment for 24 hr converted between 80 and 93 % of the Fe_3O_4 into magnetically split χ-Fe_5C_2 and some superparamagnetic component (spm) (Figure VI.4.4). The spm component appeared as a doublet with $\delta \approx 0.45$ mm/s and $\Delta \approx 1.0$ mm/s. These parameters closely match those reported for spm ϵ'-$Fe_{2.2}C$ (VI.4.7). The XRD results indicate that ϵ'-$Fe_{2.2}C$ was present for these catalysts so the spm component will be assigned as small particle ϵ'-$Fe_{2.2}C$.

In general, the catalysts containing zirconium carbided to a slightly greater extent than the unpromoted and potassium promoted catalysts. The start of synthesis gas caused the χ-Fe_5C_2 and the spm component to oxidize to Fe_3O_4 (Table VI.4.1 and Figure VI.4.5A) for all of the catalysts studied; however, the catalysts containing zirconium seemed to oxidize more slowly than the two that did not contain it.

H_2 Pretreatment. All of the catalyst series produced Fe_3O_4 during the first 6.5 hr of exposure to H_2 gas. The hyperfine fields were consistent with Fe_3O_4; however, the A and B site ratios deviated substantially from reported values (VI.4.25). Magnetite is an inverse spinel and has a B/A ratio of 2. The A site has a hyperfine field of 491 kG and the B site has a hyperfine field of 461 kG. The catalyst samples taken after 6.5 hr of pretreatment have B/A ratios ranging from 0.4 to 1.4. The low value suggests that a structure intermediate between Fe_3O_4 and γ-Fe_2O_3 may exist (VI.4.20). However, the hyperfine fields are consistent with Fe_3O_4, as is the XRD data, so this will be assigned as Fe_3O_4. Pretreatment for 24 hr produced between 17% and 28% α-Fe with the remainder being Fe_3O_4. The unpromoted catalyst reduced to the largest extent while the remaining catalysts reduced to the same level. The exposure to synthesis gas quickly converted all of the α-Fe to a mixture of ϵ'-$Fe_{2.2}C$ and what appeared to be θ-Fe_3C (Table VI.4.2). The K promoted catalysts were completely carbided after 24 hr of synthesis (Figure VI.4.5B). By the end of the runs, approximately 80% of the Fe was present as ϵ'-$Fe_{2.2}C$ with the remainder a mixture of spm ϵ'-$Fe_{2.2}C$ and θ-Fe_3C (Figure VI.4.6). The unpromoted catalyst formed carbides much more slowly; after 72 hr of synthesis, 40% of the Fe was present as Fe_3O_4. The Zr promoted

catalyst had a constant amount of Fe_3O_4 throughout its run of about 80% of the Fe (Figure VI.4.5C).

Synthesis Gas Activation. Mössbauer spectroscopy showed all of the catalysts were Fe_3O_4 after 3.5 hr of exposure to synthesis gas. The unpromoted and Zr promoted catalysts did not change throughout their runs (Table VI.4.3). The K promoted catalysts gradually carbided and by 72 hr of synthesis was 100% χ-Fe_5C_2 and ϵ'-$Fe_{2.2}C$ (Figure VI.4.5D). The doubly promoted catalyst carbided much more slowly; nevertheless, it was 85% carbide by the end of the run.

VI.4.5. DISCUSSION

The present study supports the conclusions of several others concerning the phase transformations of iron catalysts during the FT-synthesis. It was found that all four of the catalysts series that were studied rapidly converted to Fe_3O_4 during the first 3 hr of CO pretreatment. Further exposure to CO gas brought about the formation of various carbide phases. XRD data indicate the formation of χ-Fe_5C_2, ϵ'-$Fe_{2.2}C$ and possibly θ-Fe_3C. On the other hand, magnetically ordered χ-Fe_5C_2 and a substantial amount of a superparamagnetic phase, which is assigned as small particle ϵ'-$Fe_{2.2}C$, were identified from Mössbauer spectroscopy data. A similar discrepancy between XRD data and Mössbauer results has been reported where XRD identified θ-Fe_3C but Mössbauer saw only χ-Fe_5C_2 and ϵ'-$Fe_{2.2}C$ (VI.4.26). It is surprising that promotion with 0.5 atomic% K had little effect on the degree of carbide formation during the CO pretreatment. Previously it has been reported that K accelerates the conversion of Fe_3O_4 to χ-Fe_5C_2; however, it has no effect on the reduction of α-Fe_2O_3 to Fe_3O_4

(VI.4.4). For the ultrafine catalyst of this study, there was only a small difference in the content of carbides formed during the CO pretreatment.

When operating at conversions in excess of 20%, enough water vapor and CO_2 can be generated to bring about the oxidation of iron carbides to Fe_3O_4. This was seen for all of the catalysts pretreated with CO. It appears that the unpromoted and K promoted catalysts oxidized more quickly than the catalysts containing Zr. After 72 hr of synthesis all of the catalysts except the doubly promoted catalyst had greater than 90% of the iron present as Fe_3O_4; the doubly promoted catalyst had only 60% of its iron as Fe_3O_4.

Pretreatment for 24 hours in H_2 gas only partially reduced the Fe_2O_3 catalyst to metallic α-Fe. Mössbauer and XRD data confirm that the Fe_2O_3 is rapidly converted to Fe_3O_4 during the heat-up period of the pretreatment; however, further reduction of the iron to the zero valence state was much slower. The unpromoted catalyst reduced to the greatest extent with 28% of the iron present as α-Fe and the remainder as Fe_3O_4. The other three catalysts reduced to a lesser extent; 17-20% of the iron was present as α-Fe. Potassium has been reported to retard the adsorption of hydrogen on iron catalysts which would presumably inhibit iron reduction (VI.4.27). It is also possible that a layer of ZrO_2 covered some of the iron oxide surface of the Zr promoted catalysts, thereby slowing the interaction of H_2 with the catalyst particles.

Mössbauer spectroscopy and XRD data both show that the iron phase of the H_2 pretreated catalysts is converted to iron carbides during the first 3 hr of synthesis. XRD data indicate that the carbides that are formed are ϵ'-$Fe_{2.2}C$ and χ-Fe_5C_2. Mössbauer data clearly show that most of the carbide is ϵ'-$Fe_{2.2}C$; however, a smaller

component, which accounts for no more than 13% of the total Fe in any of the catalyst series, was also present. The hyperfine field for this carbide ranged from 205 to 216 kG. The literature value of the hyperfine field for θ-Fe_3C is 208±2 kG (VI.4.28) which makes cementite a good candidate for this phase. It is also possible, since only a small amount was present and the resolution of the spectra was not ideal, that this hyperfine field is the result of an averaging of the 183 kG and 219 kG sites of χ-Fe_5C_2. Potassium promotion had its greatest impact on the H_2 pretreated catalysts. The unpromoted and Zr promoted catalysts had reasonable and stable conversion (~30%); however, the K promoted catalysts deactivated very rapidly. Corresponding to this rapid deactivation was a formation of Fe carbides and a drop in surface area. Within 24 hr at synthesis conditions the doubly promoted catalyst, which showed essentially no activity, had been completely converted to Fe carbides and had a surface area of 5 m^2/g. The K promoted catalyst suffered a similar fate within 72 hr of synthesis. The catalysts that did not contain K had stable surface areas (30 m^2/g) that were only about one half that of the CO pretreated catalysts; nevertheless, their activities were about the same (30% conversion vs. ~40%) as the CO pretreated samples. This suggests that the stabilization of a high surface area is not in itself a guarantee of high conversion.

The active phase or active site of the iron based FT catalysts has been debated for years. Fischer and Tropsch initially proposed that iron carbides (VI.4.29) are the active phases while others have proposed that iron oxides such as Fe_3O_4 are active (VI.4.30). The current results of this study seem to imply that the bulk phases of the iron catalysts do not participate directly in the Fischer-Tropsch synthesis. No

apparent correlation can be made between the activity and the catalyst composition for the catalyst series activated with synthesis gas. In general, all of the catalysts of this series showed very poor activity. For the unpromoted and Zr promoted catalysts, carbide formation was not detected by either XRD or Mössbauer spectroscopy. The only bulk phase present throughout either of these runs was Fe_3O_4. The K promoted catalyst showed a high CO conversion after 24 hr of synthesis gas exposure; however, it deactivated over 72 hr to a conversion below 5%. During this time the catalyst steadily formed χ-Fe_5C_2 and ϵ -$Fe_{2.2}C$ much as this catalyst did when pretreated with H_2. Contrary to this, the doubly promoted catalyst gradually activated (maximum conversion of 27%) over the course of the run as carbide formation proceeded. This gradual activation occurred despite the decrease of surface area from 69 to 11 m^2/g. This discrepancy of surface area and activity is further exemplified by the unpromoted catalyst. This catalyst had the lowest activity of the synthesis gas activated series; nevertheless, it had the second highest surface area.

The lack of a correlation between bulk composition and activity is further supported by comparing the phase composition and activity of the K promoted catalyst that was pretreated with CO. At the start of the synthesis, the CO conversion was 32% and the iron composition was 85% χ-Fe_5C_2 and superparamagnetic carbide phase. After 72 hr of synthesis the CO conversion was essentially the same; however, the iron composition changed to 90% Fe_3O_4 and 10% superparamagnetic carbide. If bulk carbide was the active phase it would be expected that the conversion would drop and likewise if Fe_3O_4 was the active phase then the conversion should have increased. Several research groups have reported evidence of a surface carbidic species being responsible for FT activity (VI.4.31,VI.4.32). It is possible that the bulk

phases act as supports for active surface species and may play an indirect role in the activity of iron based catalysts.

To summarize, four major conclusions can be made about the ultrafine Fe_2O_3 catalyst. Pretreatment in CO is superior to H_2 or synthesis gas in terms of overall synthesis gas conversion and stability. The pretreatment type seems to have a larger impact on the catalyst performance than the presence of K and/or Zr promoters. High surface area does not necessarily correlate with high activity, but may be more closely related to the concentration of surface active sites. The activity of iron based catalysts is not dependent on the bulk phases.

VI.4.6. ACKNOWLEDGMENT

This work was supported by funding from the U.S. Department of Energy through Contract No. DE-AC22-90PC90049 and the Commonwealth of Kentucky.

VI.4.7. REFERENCES

1. M. E. Dry, in: *Catalysis-Science and Technology*, Vol 1, eds. J. R. Anderson and M. Boudart (Springer-Verlag, New York, 1981) ch. 4.
2. R. B. Anderson; in: *Catalysis* , Vol 4, ed. P. H. Emmett (Rheinhold Pub. Corp., New York, NY, 1956) pp. 29-255.
3. D. B. Bukur, D. Mukesh, S. A. Patel, *Ind. Eng. Chem. Res.* 29 (1990) 194.
4. F. J. Berry, M. R. Smith, *J. Chem. Soc. Faraday Trans.* 85 (1989) 467.
5. M. E. Dry, G. J. Oosthuizen, *J. Catal.* 11 (1968) 18.
6. D. B. Bukur, X. Lang, D. Mukesh, W. H. Zimmerman, M. P. Rosynek, C: Li, *Ind. Eng. Chem. Res.* 29 (1990) 1588.
7. J. A. Amelse, J. B. Butt, L. H. Schwartz, *J. Phys. Chem.* 82 (1978) 558.
8. D. B. Bukur, X. Lang, J. A. Rossin, W. H. Zimmerman, M. P. Rosynek, E. B. Yeh, C. Li, *Ind. Eng. Chem. Res.* 28 (1989) 1130.
9. M. F. Zarochak, M. A. McDonald, *Proc. Indirect Liquefaction Contractors' Meeting*, 1986, Pittsburgh, p. 58.
10. H. Abrevaya, P. Shah, *Proc. Indirect Liquefaction Contractors' Meeting*, 1990, Pittsburgh, p. 203.
11. J. T. McCartney, L. J. E. Hofer, B. Seligman, J. A. Lecky, W. C. Peebles, R. B. Anderson, *J. Phys. Chem.* 57 (1953) 730.
12. G. Le Caer, J. M. Dubois, M. Pijolat, V. Perrichon, P. Bussière, *J. Phys. Chem.* 86 (1982) 4799.
13. H. C. Eckstrom, W. A. Adcock, *J. Am. Chem. Soc.* 72 (1950) 1042.

14. R. B. Anderson, *The Fischer-Tropsch Synthesis*, (Academic Press, Orlando, Florida, 1984).

15. H. Itoh, H. Hosaka, T. Ono, E. Kikuchi, *Appl. Catal.* 40 (1988) 53.

16. H. Itoh, E. Kikuchi, *Appl. Catal.* 67 (1990) 1.

17. H. Itoh, S. Nagano, E. Kikuchi, *Appl. Catal.* 67 (1991) 215.

18. H. Itoh, S. Nagano, T. Urata, E. Kikuchi, *Appl. Catal.* 77 (1991) 37.

19. C.-S. Huang, L. Xu, B. H. Davis, *Fuel Sci. & Technol. Int.* 11 (1993) 639.

20. C.-S. Huang, B. Ganguly, G. P. Huffman, F. E. Huggins, B. H. Davis, *Fuel Sci. & Technol. Int.*, 11 (1993) 1289.

21. L.-M. Tau, H. A. Dabbagh, T. P. Wilson, B. H. Davis, *Appl. Catal.* 56 (1989) 95.

22. H. H. Storch, N. Golumbic, R. B. Anderson: *The Fischer-Tropsch and Related Synthesis* (John Wiley, New York, 1951).

23. P. Ganesan, B. H. Davis, *Ind. Eng. Chem., Prod. Res. & Dev.* 18 (1979) 191.

24. W. S. Brey, B. H. Davis, *J. Catal.* 25 (1972) 81.

25. H. Topsφe, M. Boudart, *J. Catal.* 31 (1973) 346.

26. E. S. Lox, G. B. Marin, E. De Grave, P. Bussière, *Appl. Catal.* 40 (1988) 197.

27. M. E. Dry, T. Shingle, L. J. Boshoff, G. J. Oosthuizen, *J. Catal.* 15 (1969) 190.

28. H. Bernas, I. A. Campbell, R. Fruchart, *J. Phys. Chem. Solids* 28 (1967) 17.

29. F. Fischer, H. Tropsch, *Brenstoff-Chem.* 7 (1926) 97.

30. J. P. Reymond, P. Mériaudeau, S. J. Teichner, *J. Catal.* 75 (1982) 39.

31. P. Biloen, J. N. Helle, W. M. H. Sachtler, *J. Catal.* 58 (1979) 95.

32. H.-B. Zhang, G. L. Schrader, *J. Catal.* 95 (1985) 325.

Table VI.4.1

Mössbauer Spectral Composition of CO Pretreated Catalysts at Various Times of the Fischer-Tropsch Synthesis

Catalyst	Time of Synthesis, hr	$CO + H_2$ Conversion, %	Fe Composition, %
100 Fe	0		M(20), χ(47), S(33)
	3	39	M(37), χ(36), S(28)
	72	30	M(91), S(9)
100 Fe/0.5 K	0		M(11), χ(45), S(43)
	3	32	M(36), χ(32), S(32)
	24	23	M(64), χ(20), S(16)
	72	28	M(88), S(12)
100 Fe/1.0 Zr	0		M(7), χ(54), S(39)
	3.5	52	M(12), χ(52), S(35)
	24	64	M(33), χ(41), S(26)
	72	44	M(91), S(9)
100 Fe/0.5 K/1.0 Zr	0		M(14), χ(52), S(34)
	3.5	29	M(16), χ(51), S(33)
	24	42	M(35), χ(42), S(24)
	72	37	M(60), χ(21), S(19)

M = Fe_3O_4, χ = χ-Fe_5C_2, S = superparamagnetic carbide

Table VI.4.3

Mössbauer Spectral Composition of $CO+H_2$ Activated Catalysts at Various Times of the Fischer-Tropsch Synthesis

Catalyst	Time of Synthesis, hr	$CO + H_2$ Conversion, %	Fe Composition, %
100 Fe	3.5	4	M(100)
	24	6	M(100)
	48	7	M(100)
	72	6	M(100)
100 Fe/0.5 K	0		M(70), ϵ'(19), χ(12)
	24	26	M(14), ϵ'(31), χ(54)
	72	4	ϵ'(42), χ(53), S(5)
100 Fe/1.0 Zr	0		M(100)
	24	< 3	M(100)
	48	< 3	M(100)
	72	< 3	M(100)
100 Fe/0.5 K/1.0 Zr	0		M(100)
	24	7	M(96), ϵ'(2), χ(2)
	48	10	M(64), ϵ'(15), χ(16), S(5)
	72	18	M(17), ϵ'(34), χ(43), S(6)

M = Fe_3O_4, χ = χ-Fe_5C_2, ϵ' = ϵ'-$Fe_{2.2}C$, S = superparamagnetic carbide

Table VI.4.2

Mössbauer Spectral Composition of H_2 Pretreated Catalysts at Various Times of the Fischer-Tropsch Synthesis

Catalyst	Time of Synthesis, hr	CO + H_2 Conversion, %	Fe Composition, %
100 Fe	0		M(72), Fe(28)
	3.5	34	M(75), ϵ'(10), θ(6), S(9)
	24	26	M(79), ϵ'(11), θ(6), S(5)
	71	39	M(47), ϵ'(28), θ(14), S(11)
100 Fe/0.5 K	0		M(83), Fe(17)
	3.5	18	M(41), ϵ (43), θ(10), S(2)
	24	4	ϵ'(79), θ(9), S(12)
100 Fe/1.0 Zr	0		M(83), Fe(17)
	3.5	27	M(93), ϵ'(4), θ(1), S(2)
	24	22	M(82), ϵ'(15), θ(2), S(1)
	71	25	M(79), ϵ'(10), θ(1), S(10)
100 Fe/0.5 K/1.0 Zr	0		M(80), Fe(20)
	3.5	10	M(60), ϵ'(32), θ(2), S(5)
	24	3	ϵ'(88), θ(4), S(8)
	72	6	ϵ (79) θ(8), S(13)

M = Fe_3O_4, ϵ' = ϵ'-$Fe_{2.2}C$, θ = θ-Fe_3C, S = superparamagnetic carbide

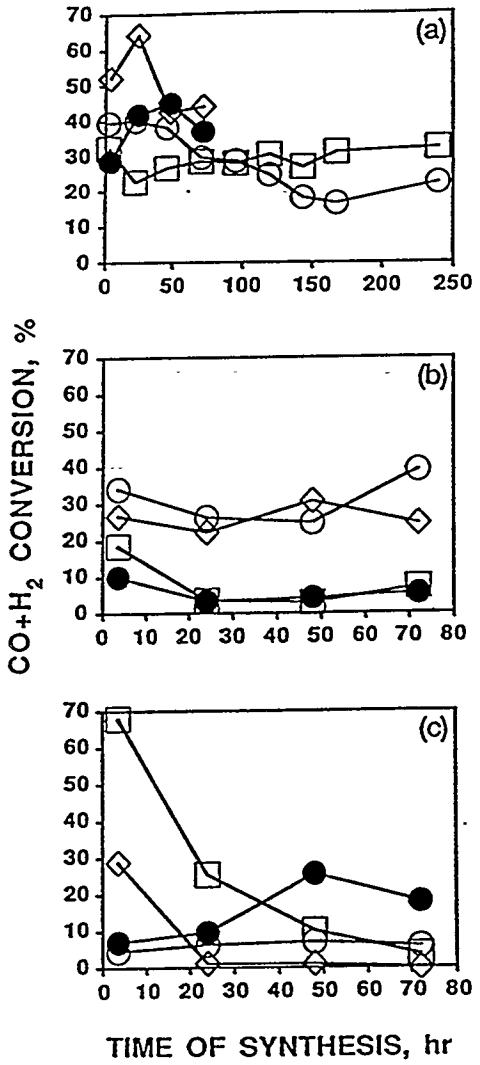

Figure VI.4.1. Synthesis gas conversion for (a) catalysts pretreated with CO, (b) pretreated with H_2, and (c) activated with synthesis gas, $H_2/CO=1.0$. ○ - 100Fe, □ - 100Fe/0.5K, ◇ - 100Fe/1.0Zr, ● - 100Fe/0.5K/1.0Zr.

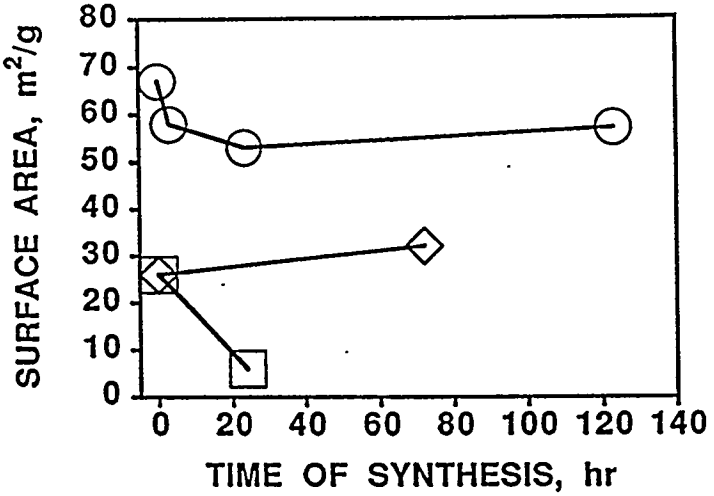

Figure VI.4.2. Change in surface area of 100Fe/0.5K catalyst during synthesis. ○ - pretreated with CO, □ - pretreated with H_2 and ◇ - activated with synthesis gas, $H_2/CO=1$.

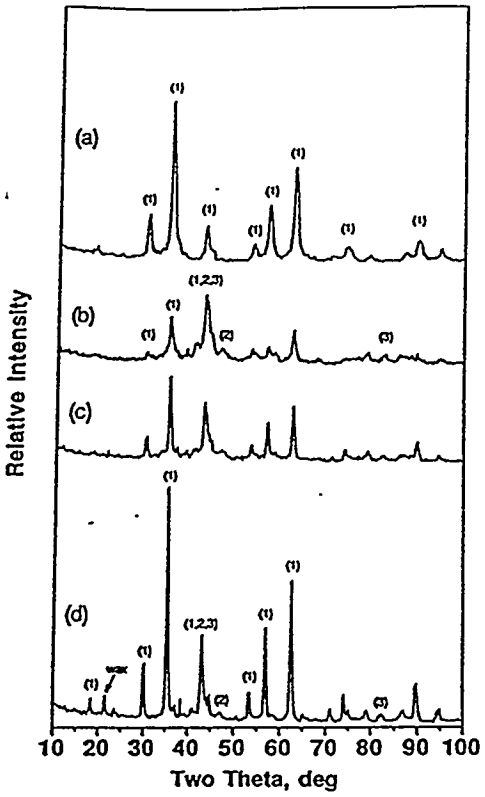

Figure VI.4.3. X-ray diffraction patterns of 100Fe/0.5K/1.0Zr catalyst following (a) 3 hr and (b) 24 hr of CO pretreatment and (c) 24 hr and (d) 72 hr of FT synthesis at 260°C, 8 atm, H_2/CO = 1.0, 3.0 nL/hr/g(Fe). (1)- Fe_3O_4, (2)- χ-Fe_5C_2, (3)-ϵ'-$Fe_{2.2}C$.

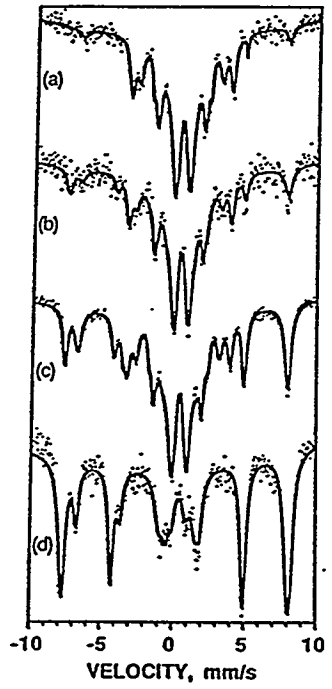

Figure VI.4.4. Mössbauer spectra of 100Fe/1.0Zr catalyst following (a) 24 hr of CO pretreatment and following (b) 3 hr, (c) 24 hr, and (d) 72 hr of FT synthesis at 260°C, 8 atm, H_2/CO = 1.0, 3.0 nL/hr/g(Fe).

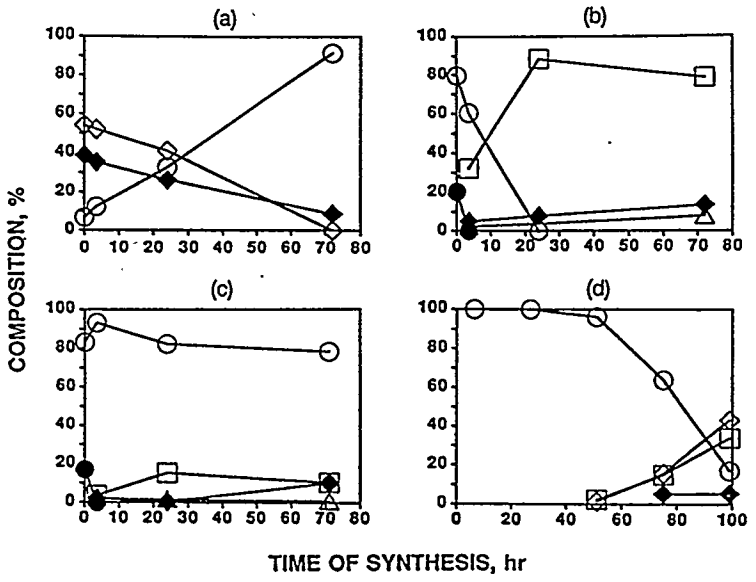

Figure VI.4.5. Compositional changes of (a) 100Fe/1.0Zr catalyst pretreated with CO, (b) 100Fe/0.5K/1.0Zr catalyst pretreated with H_2, (c) 100Fe/1.0Zr catalyst pretreated with H_2 and (d) 100Fe/0.5K/1.0Zr catalyst activated in synthesis gas, $H_2/CO = 1.0$. ○ - Fe_3O_4, ◇ - χ-Fe_5C_2, □ - ϵ'-$Fe_{2.2}C$, △ -θ-Fe_3C, ◆ - spm carbide, ● - Fe.

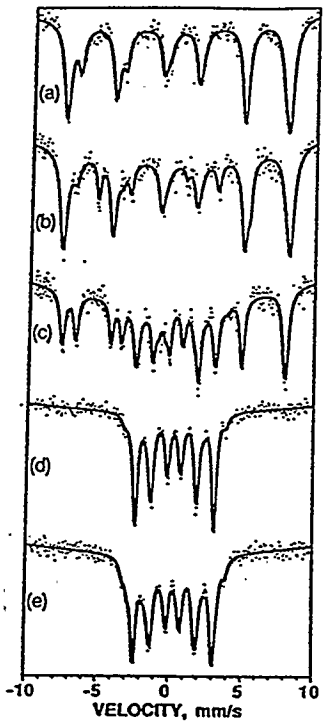

Figure VI.4.6. Mössbauer spectra of 100Fe/0.5K/1.0Zr catalyst following (a) 3 hr and (b) 24 hr of H_2 pretreatment and following (c) 3 hr, (d) 24 hr and (e) 72 hour of FT synthesis at 260°C, 8 atm, $H_2/CO = 1.0$, 3.0 nL/hr/g(Fe).